Earth and Planetary Science Letters 376 (2013) 43–53

Contents lists available at ScienceDirect

Earth and Planetary Science Letters

www.elsevier.com/locate/epsl

Diet and environment of a mid-Pliocene fauna from southwestern Himalaya: Paleo-elevation implications

Yang Wang [a,b,*], Yingfeng Xu [a,b], Sofia Khawaja [a,b], Benjamin H. Passey [c], Chunfu Zhang [a,b,h], Xiaoming Wang [d,e], Qiang Li [e], Zhijie J. Tseng [d], Gary T. Takeuchi [f], Tao Deng [e], Guangpu Xie [g]

[a] Department of Earth, Ocean & Atmospheric Science, Florida State University, Tallahassee, FL 32306, USA
[b] National High Magnetic Field Laboratory, Tallahassee, FL 32306-4100, USA
[c] Department of Earth and Planetary Sciences, Johns Hopkins University, Baltimore, MD 21218, USA
[d] Department of Vertebrate Paleontology, Natural History Museum of Los Angeles County, Los Angeles, CA 90007, USA
[e] Institute of Vertebrate Paleontology and Paleoanthropology, Chinese Academy of Sciences, Beijing, PR China
[f] The George C. Page Museum of La Brea Discoveries, 5801 Wilshire Blvd., Los Angeles, CA 90036, USA
[g] Gansu Provincial Museum, Lanzhou 730050, PR China
[h] Department of Geosciences, Fort Hays State University, Hays, KS 67601, USA

ARTICLE INFO

Article history:
Received 3 January 2013
Received in revised form 7 May 2013
Accepted 10 June 2013
Available online 28 June 2013
Editor: T.M. Harrison

Keywords:
stable isotopes
paleo-diet
paleo-temperature
paleo-elevation
Himalaya
Tibetan Plateau

ABSTRACT

A mid-Pliocene fauna (4.2–3.1 Ma) was recently uncovered in the Zanda (Zhada) Basin in the southwestern Himalaya, at an elevation of about 4200 m above sea level. These fossil materials provide a unique window for examining the linkage among tectonic, climatic and biotic changes. Here we report the results from isotopic analyses of this fauna and of modern herbivores and waters as well as paleo-temperature estimates from the Zanda Basin. The $\delta^{13}C$ values of enamel samples from modern wild Tibetan asses, and domesticated horses, cows and goats in the area are $-9.4 \pm 1.8‰$, which indicate a diet comprising predominantly of C_3 plants and are consistent with the current dominance of C_3 vegetation in the region. The enamel-$\delta^{13}C$ values of the fossil horses, rhinos, deer, and bovids are $-9.6 \pm 0.8‰$, indicating that these ancient mammals, like modern herbivores in the area, also fed primarily on C_3 vegetation and lived in an environment dominated by C_3 plants. The lack of significant C_4 plants in the basin suggests that the area had reached high elevations (>2.5 km) by at least the mid-Pliocene. Taking into account the changes in the $\delta^{13}C$ of atmospheric CO_2 in the past, the enamel-$\delta^{13}C$ values suggest that the average modern-equivalent $\delta^{13}C$ value of C_3 vegetation in the Zanda Basin in the mid-Pliocene was ~1–2‰ lower than that of the C_3 biomass in the basin today. This would imply a reduction in annual precipitation by about 200–400 mm in the area since then (assuming that the modern C_3 $\delta^{13}C$–precipitation relationship applied to the past). Consistent with this inference from the $\delta^{13}C$ data, the enamel-$\delta^{18}O$ data show a significant shift to higher values after the mid-Pliocene, which also suggests a shift in climate to much drier conditions after ~4–3 Ma.

Paleo-temperature estimates derived from a fossil bone-based oxygen isotope temperature proxy as well as the carbonate clumped isotope thermometer for the mid-Pliocene Zanda Basin are higher than the present-day mean annual temperature in the area. After accounting for late Cenozoic global cooling, these paleo-temperature estimates suggest that the paleo-elevation of the Zanda Basin in the mid-Pliocene was similar to or slightly (less than ~1 km) lower than its present-day elevation, which is consistent with the inference from the $\delta^{13}C$ data.

1. Introduction

The uplift of the Himalayan–Tibetan Plateau has been suggested to be a major driving mechanism of regional and global climate change during the late Cenozoic (An et al., 2001; Harrison et al., 1992; Molnar, 2005; Molnar et al., 1993; Raymo and Ruddiman, 1992; Ruddiman et al., 1997). However, local environmental changes within the Tibetan region could also be caused by global climate change (Dupont-Nivet et al., 2007; Wang et al., 2012). Teasing apart the effects of tectonic and global climatic changes on local environments within the Himalayan–Tibetan Plateau is difficult and, as a result, the timing of the Tibetan uplift remains a hotly

* Corresponding author at: Department of Earth, Ocean & Atmospheric Science, Florida State University, Tallahassee, FL 32306, USA. Tel.: +1 850 644 1121; fax: +1 850 644 0827.
E-mail address: ywang@magnet.fsu.edu (Y. Wang).

http://dx.doi.org/10.1016/j.epsl.2013.06.014
0012-821X

debated issue. Uplift histories of the Himalayan–Tibetan Plateau based on different proxies differ considerably (Currie et al., 2005; Cyr et al., 2005; DeCelles et al., 2007; Dupont-Nivet et al., 2008; Garzione et al., 2000; Graham et al., 2005; Harrison et al., 1992; Li and Zhou, 2001, 2002; Meng et al., 2004; Murphy et al., 2009; Quade et al., 2011; Rowley and Currie, 2006; Rowley et al., 2001; Saylor et al., 2010b, 2009; Spicer et al., 2003; Sun et al., 2007; Wang et al., 2006, 2012, 2008b; Xu et al., 2012). For example, oxygen isotope paleoaltimetry studies (based on the oxygen isotopic compositions of lake and paleosol carbonates) suggest that southern Tibet has been as high as today or higher since at least the mid-Miocene and perhaps as early as the late Eocene (Rowley and Currie, 2006; Rowley and Garzione, 2007). In contrast, paleofloral assemblages and clay mineralogy preserved in basin-fill sediments on the Tibetan Plateau are similar to modern assemblages in warm, low elevation environments and have been used to argue for significant uplift of 1–2 km since the late Miocene (Li and Zhou, 2001, 2002; Meng et al., 2004; Sun et al., 2007; Wang et al., 2006, 2012; Xu, 1981; Xu et al., 2012; Zhang et al., 1981).

A mid-Pliocene (4.2–3.1 Ma) fauna containing a primitive woolly rhino was recently discovered in the Zanda (Zhada) Basin in western Himalaya, at an elevation of about 4200 m above sea level (Deng et al., 2011). These fossil materials, along with abundant fossil shells found in the same basin (Saylor et al., 2009), are archives of paleoenvironments. Specifically, carbon and oxygen isotopic compositions of fossil tooth enamel and bones contain valuable information about the diet and water isotopic composition, and paleo-temperature (Cerling et al., 1997; Kohn and Law, 2006; Wang et al., 2008a, 2008b; Zanazzi et al., 2007). Fossil shells on the other hand are a recorder of lake water isotopic composition and temperature, which are controlled by regional hydrology and climate.

In this study, we analyzed the carbon and oxygen isotopic compositions of 307 serial and bulk enamel samples from a diverse group of fossil and modern herbivores as well as the oxygen and hydrogen isotopic compositions of precipitation and stream waters from the Zanda Basin in the southwestern Tibetan Plateau to examine the diet and environmental changes in the area since the mid-Pliocene. We also estimated paleo-temperatures in the basin in the mid-Pliocene using two different paleo-temperature methods – the carbonate clumped isotope thermometry (Ghosh et al., 2006) and a fossil-based oxygen isotope temperature proxy (Kohn and Law, 2006; Zanazzi et al., 2007). Our results provide new insights into the environmental and tectonic evolution of the area from the mid-Pliocene to the present.

2. Study area

The Zanda Basin (~31°N, ~80°E) is the largest Neogene sedimentary basin in the western Himalayan orogen (Saylor et al., 2010a, 2010b). It is located just north of the high Himalayan ridge crest in southwestern Tibet (Fig. 1). The basin is ~260 km long and ~60 km wide, extending roughly in the NW–SE direction (Saylor et al., 2010b). The current elevation of the basin is ~3700–4500 m above sea level (a.s.l.). The basin is bounded by the South Tibetan Detachment System to the southwest, the Leo Pargil to the northwest, the Indus suture to the northeast and Gurla Mandhata gneiss domes to the southeast (Saylor et al., 2010b). Its tectonic origin is uncertain although various models have been proposed (Zhou et al., 2000; Wang, 2004; Saylor et al., 2010a).

The present-day Zanda Basin is characterized by cold and dry climatic conditions. The landscape in the area consists mostly of desert and cold steppe with grasses and short shrubs. The mean annual temperature (MAT) in the Zanda area is about 0–3 °C and the annual precipitation is ~200 mm (Li and Zhou, 2002; Li, 2006). Summer temperatures are about 13–14 °C, with maximum summer temperatures reaching as high as 21 °C; whereas winter temperatures can reach −41 °C (Li, 2006). Summer monsoon rainfalls account for most of the annual precipitation and come primarily in June–August; whereas winter and spring snow storms are possibly associated with westerly winds (Li, 2006; Tian et al., 2001, 2005).

The Zanda Basin contains thick (>800 m) deposits of Mio-Pleistocene fluvial, lacustrine, and alluvial fan sediments – the Zanda Formation (Fig. 2), which has abundant gastropod shells, fish, and mammalian fossils. The Zanda Formation forms an angular unconformity with the underlying Tethyan strata that were previously deformed in the Himalayan fold-thrust belt (Saylor et al., 2010b). Fossil mammals are the most abundant in the middle section where most samples were collected in this study (Wang et al., 2013). The ages of the fossils were determined on the basis of correlation of stratigraphic positions of fossil localities with the paleomagnetic stratigraphy using fossil mammals as constraints for correlation to the Geomagnetic Polarity Time Scale (GPTS) (Fig. 2; Wang et al., 2013; Saylor et al., 2009).

3. Materials and methods

We obtained 235 serial and bulk enamel samples from 74 teeth or tooth fragments from a diverse group of mid-Pliocene mammals (including horse, rhino, deer, and bovid) for stable carbon (C) and oxygen (O) isotope analyses of structural carbonate in bioapatite. In addition, we analyzed the C and O isotopic compositions of 60 bulk and serial enamel samples from 14 modern teeth from 7 Tibetan wild asses (*Equus kiang*), 2 domestic horses (*Equus caballus*), 2 domestic cows (*Bos primigenius*) and 3 domestic goats (*Capra hircus*) from the Zanda Basin. These modern teeth were extracted either from decaying carcasses or from partial skeletons of recently deceased animals found in the field. Some are individual teeth collected outside villages. Mammalian fossils were mostly collected from alluvial sediments and near-shore lacustrine/fluvial sediments. All teeth and bones were cleaned by scraping any dirt or other material off the enamel. Bulk enamel samples were taken by drilling down the tooth along the growth axis. Serial samples were collected by drilling in bands perpendicular to the growth axis. Bones were ground into powder using a mortar and pestle. The enamel and bone powders were soaked in 5% sodium hypochlorite (NaOCl) overnight to remove any possible organic contaminants, cleaned with distilled water and freeze-dried. The powder was then treated with 1 M acetic acid overnight to remove carbonate, cleaned with distilled water and freeze-dried (Wang and Deng, 2005). The treated enamel and bone samples were reacted with anhydrous phosphoric acid at 25 °C for about 72 h and the carbon and oxygen isotopic ratios of the CO_2 produced were measured using a Gas Bench II Auto-carbonate device connected to a Finnigan MAT Delta Plus XP stable isotope ratio mass spectrometer (IRMS) at the Florida State University. Water samples were analyzed using the equilibration methods (Thermo Finnigan Operating Manual). 500 microliters (μL) of water were injected into an open vial and then a platinum catalyst rod was inserted in the vial. The vial was then sealed with a new septum. Vials containing water samples and standards were then flushed with helium containing 2% H_2 (which was used as an equilibration gas). Hydrogen isotope measurements were carried out after an equilibration time of 40 min (at 25 °C) using the Gas Bench II Auto-carbonate/water device connected to the IRMS. After the hydrogen isotope analysis was completed, the vials containing the samples and standards were flushed with He containing 0.3% CO_2 (as an equilibration gas), and the oxygen isotope ratios of the CO_2 were analyzed after an equilibration time of 24 h at 25 °C. Results are reported in standard delta (δ) notation as $\delta^{13}C$,

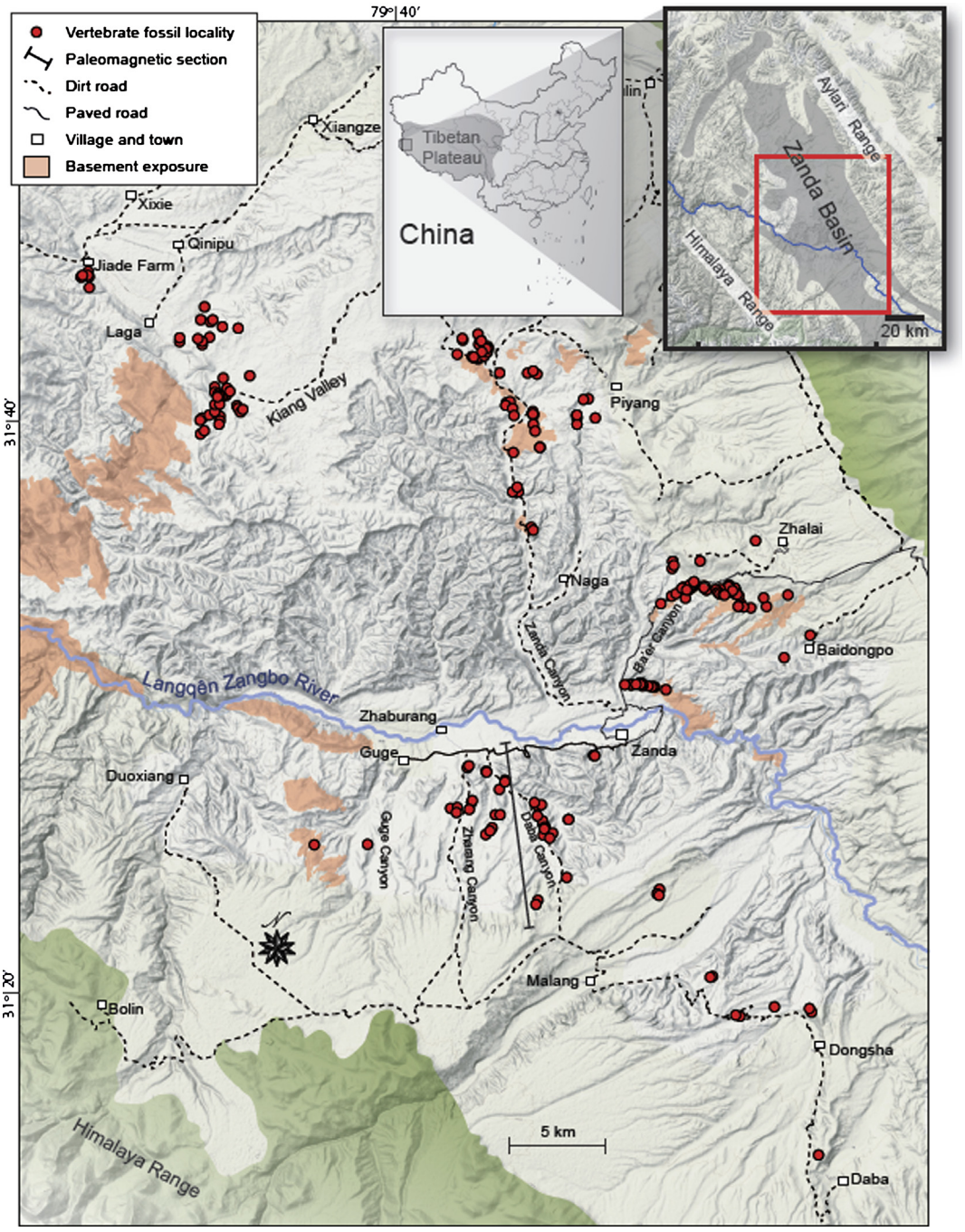

Fig. 1. Map showing the fossil localities in the Zanda Basin in southwestern Tibet, China (modified from Wang et al., 2013). The base map is from Google Earth (Version 6.1.0.5001, 2011). (Available from http://www.google.com/earth/download/ge/agree.html, Google Inc., Mountain View, CA.)

$\delta^{18}O$ and δD values in reference to the international carbonate standard VPDB and water standard VSMOW. The analytical precision (based on replicate analyses of NBS-19 and VSMOW and several other lab standards processed with each batch of samples) is $\pm 0.1‰$ or better for both $\delta^{13}C$ and $\delta^{18}O$, and $\pm 1‰$ for δD.

Selected fossil shells (freshwater snails) from lacustrine sediments were analyzed for determination of clumped isotope (Δ_{47}) temperatures. Fossil shells were cleaned in a weak HCl solution (<1%) in an ultrasonic bath, rinsed with DI water, and air-dried. The cleaned shells were then ground into powder. Analyses were conducted at the California Institute of Technology using methods described in Passey et al. (2010). The samples were reacted in anhydrous H_3PO_4 at 90 °C, and the resultant CO_2 was purified cryogenically and by passage through a Porapak-Q GC column held at −10 °C. Mass 44–49 isotopologue ratios were measured using a Thermo MAT 253 mass spectrometer, and the data were reduced using the scheme detailed in Huntington et al. (2009). An acid temperature correction factor of +0.081‰ was applied to all data to normalize values to 25 °C reactions (Ghosh et al., 2006; Passey et al., 2010). All data are reported relative to the 'heated gas' scale (e.g., Ghosh et al., 2006; Huntington et al., 2009), since they were analyzed prior to conception of the 'absolute reference frame' proposed by Dennis et al. (2011).

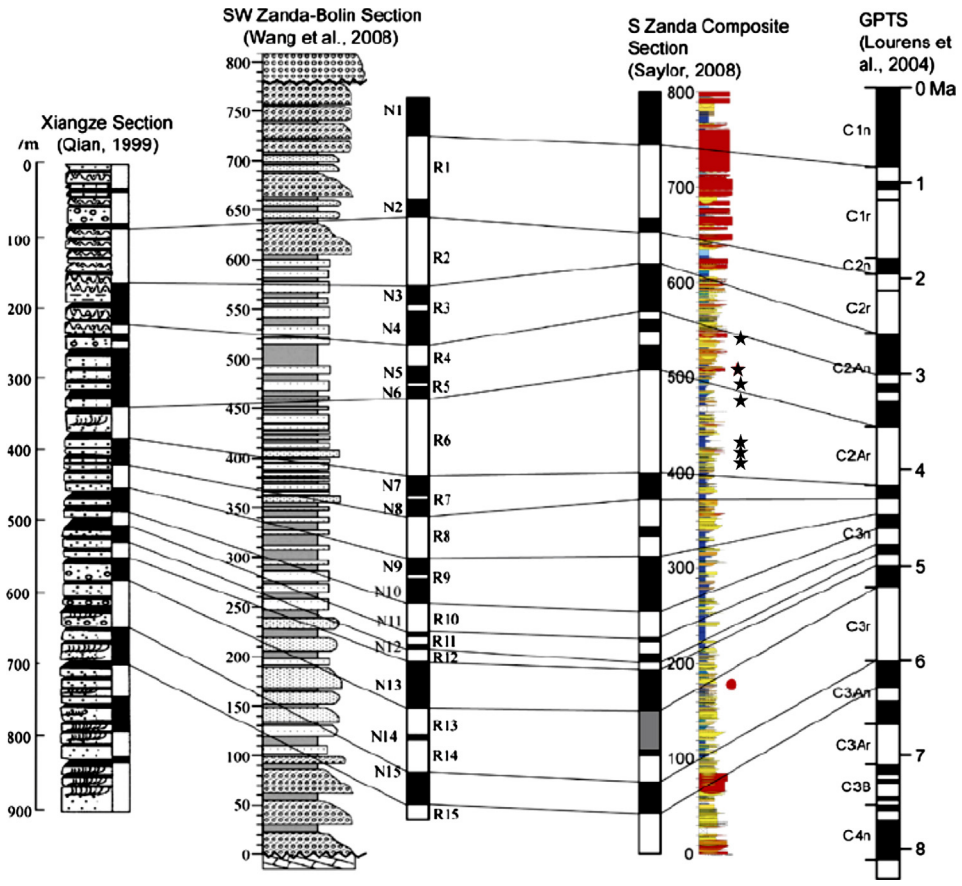

Fig. 2. Litho- and magneto-stratigraphy in the Zanda Basin and stratigraphic positions of key fossil mammal localities (modified from Deng et al., 2011: Fig. S3). Vertebrate fossils are placed in the nearest measured sections by Saylor et al. (2010b), which are in turn correlated on the basis of intrabasin sequence stratigraphic criteria. Key fossil sites are indicated by stars and red dot. Ages for magnetic chrons in the Geomagnetic Polarity Time Scale (GPTS) are based on ATNTS2004 in Lourens et al. (2004).

4. Results and discussion

4.1. Carbon isotopes and diets of the mid-Pliocene fauna

Carbon isotopic composition of tooth enamel from herbivores reflects the proportion of C_3 and C_4 plants in their diet. C_3 plants, which include all trees, cool season grasses, and most shrubs, have $\delta^{13}C$ values ranging from $-20‰$ to $-35‰$, with a mean of $-27‰$ (Cerling et al., 1997; Kohn, 2010; O'Leary, 1988). Under water-stressed conditions and/or low atmospheric partial pressure of CO_2 (pCO_2), C_3 plants are less depleted in ^{13}C and have $\delta^{13}C$ values higher than the average value of $-27‰$. Under closed canopies, C_3 plants have lower $\delta^{13}C$ values ($< -27‰$) due to the influence of soil respiration and light limitation (Cerling et al., 1997; Kohn, 2010). C_4 plants are mostly warm climate grasses and have $\delta^{13}C$ values of $-9‰$ to $-17‰$, averaging $-13‰$ (Cerling et al., 1997; O'Leary, 1988). Because tooth enamel is consistently enriched in ^{13}C by $\sim 14‰$ relative to the diet due to biochemical fractionation, animals that eat C_3 vegetation typically have $\delta^{13}C$ values less than $-9‰$; animals that eat C_4 plants have $\delta^{13}C$ values $> -2‰$; and mixed feeders that eat both fall somewhere in between these two extremes (e.g., Cerling et al., 1997). In much of the modern Himalayan–Tibetan Plateau, which is characterized by high aridity (i.e., severe water-stressed conditions) and low atmospheric pCO_2, the conservative "cut-off" enamel-$\delta^{13}C$ value for a pure C_3 diet for modern herbivores is $-8‰$ (Wang et al., 2008a).

The fossils recently uncovered in the Zanda Basin suggest a rich and diverse fauna in the area in the mid-Pliocene (Wang et al., 2013). In contrast, the modern fauna on the Himalayan–Tibetan plateau is characterized by a low number and low diversity of mammals. The only large mammals in the area today are wild Tibetan asses (*Equus kiang*; in limited but unknown number), Tibetan gazelle (*Procapra picticaudata*), blue sheep (or bharal) (*Pseudois nayaur*), extremely rare Tibetan antelopes (Chiru) (*Pantholops hodgsoni*), and some domesticated animals such as cows, goats and yaks. The average $\delta^{13}C$ value of enamel samples from modern wild Tibetan asses and domesticated herbivores (including horses, cows and goats) from the Zanda Basin is $-9.4 \pm 1.8‰$ ($n = 14$, all means reported ± 1 standard deviation σ), which corresponds to a dietary $\delta^{13}C$ value of $-23.4 \pm 1.8‰$ and is within the range of a pure C_3 diet in dry ecosystems (Kohn, 2010; Wang et al., 2008a). This indicates that modern herbivores from the Zanda Basin fed primarily on C_3 plants experiencing severe water stress, consistent with the present-day cold and arid environment in the area. The enamel-$\delta^{13}C$ values for the time period of 4.2–3.1 Ma are $-9.5 \pm 0.8‰$ ($n = 74$). The $\delta^{13}C$ of atmospheric CO_2 in the mid-Pliocene was about $-6.4‰$ (Tipple et al., 2010), which is $1.8‰$ higher than the present-day atmospheric CO_2 $\delta^{13}C$ value of $-8.2‰$ (Cuntz, 2011). After correcting for the change in the $\delta^{13}C$ of atmospheric CO_2 ($1.8‰$) and the biochemical fractionation between enamel and diet ($\sim 14‰$), the enamel-$\delta^{13}C$ values of the mid-Pliocene herbivores from the Zanda Basin are equivalent to a modern dietary intake of $-25.3 \pm 0.8‰$, well within the $\delta^{13}C$ range of modern C_3 plants. This indicates that these ancient herbivores fed primarily on C_3 vegetation and lived in an environment dominated by C_3 plants (Fig. 3a). Only a single 4.1-Ma bovid and three modern domesticated animals (a cow, a goat and a horse) yielded enamel-$\delta^{13}C$ values slightly higher than $-8‰$ (Fig. 3a), suggesting that they may have consumed a small amount of C_4 plants

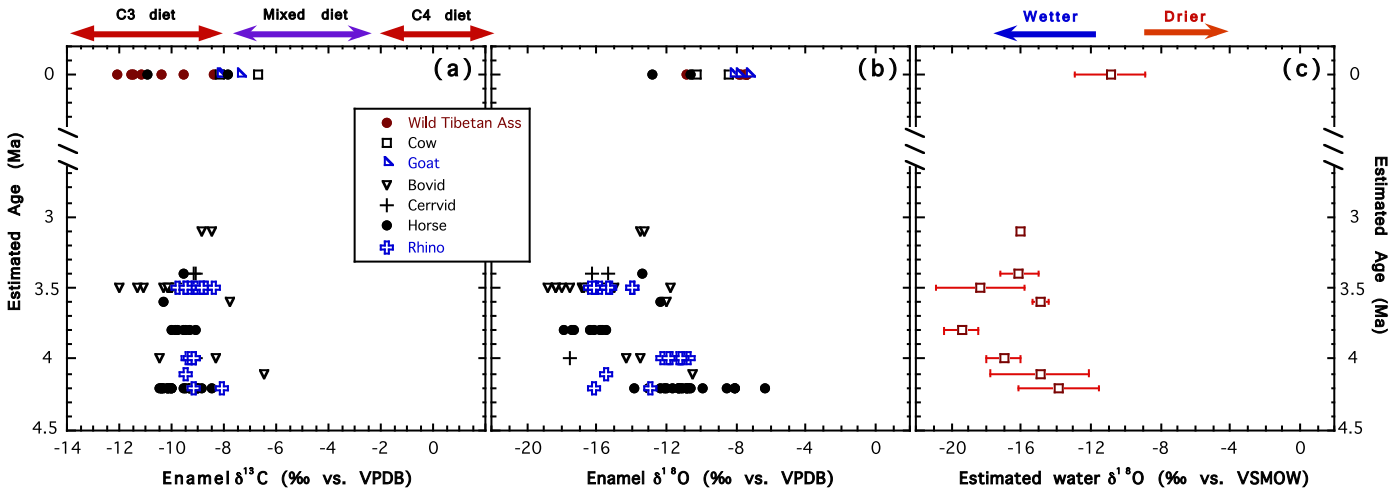

Fig. 3. Temporal variations of bulk enamel-$\delta^{13}C$ (a) and $\delta^{18}O$ values (b) of herbivores, and (c) $\delta^{18}O$ of local water estimated from the enamel-$\delta^{18}O$ values of large mammals (horse, rhino, bovid and cow) in the Zanda Basin since ~4.2 Ma. The uncertainty in the water $\delta^{18}O$ estimates corresponds to 1 sigma (1σ) standard deviation in $\delta^{18}O$ of enamel. The data show that herbivores in the Zanda Basin have had C_3-based diets since ~4.2 Ma, except one 4.1 Ma bovid and three modern domesticated animals (a cow, a horse and a goat) that may have consumed a small amount of C_4 plants. The positive shift in the estimated $\delta^{18}O$ of local water likely indicates a shift in climate to much drier conditions after ~4–3 Ma.

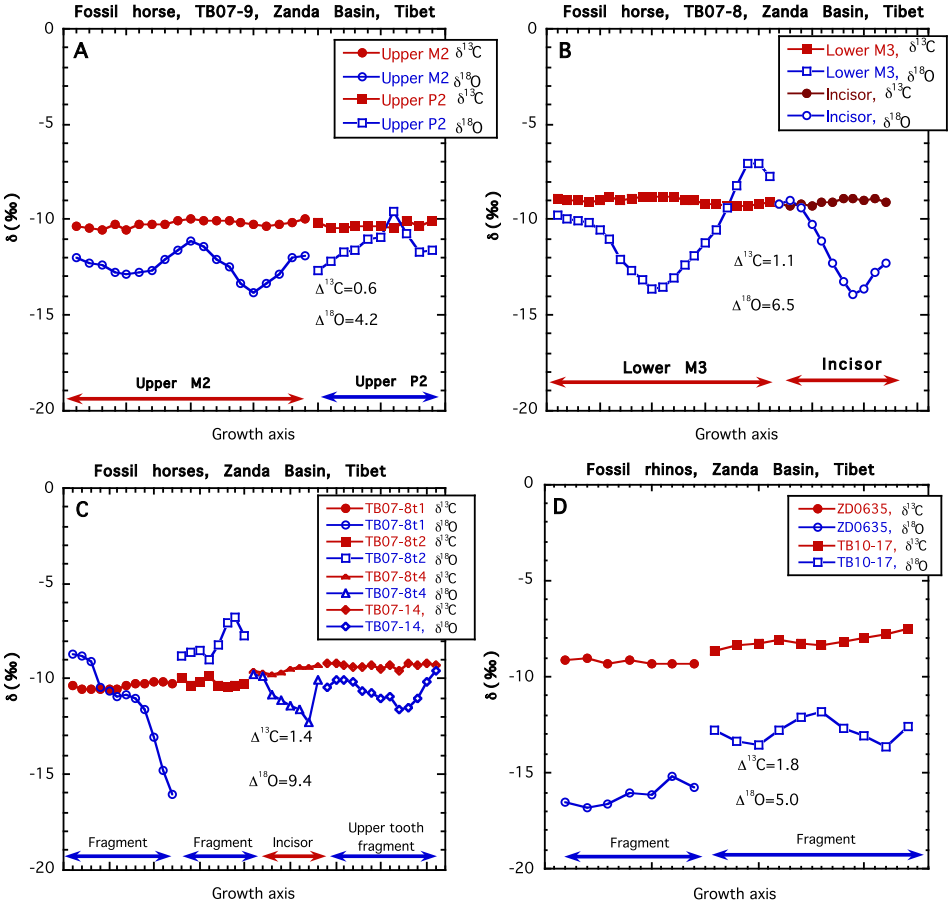

Fig. 4. Composite seasonal $\delta^{13}C$ (solid/red symbols) and $\delta^{18}O$ (open/blue symbols) records from 4.2 Ma herbivores in Zanda Basin, Tibet: (A) profiles of an upper M2 and an upper P2 of a *Hipparion* horse, (B) profiles of a lower M3 and an incisor from a *Hipparion* horse, (C) profiles of tooth fragments and an incisor from fossil horses, and (D) profiles of tooth fragments from rhinos. Each composite record represents more than 2 annual cycles. The lack of significant intra-tooth $\delta^{13}C$ variations indicates that there were little or no seasonal variations in the diets of these ancient herbivores and their diets consisted exclusively of C_3 plants.

(<15% C_4 assuming end-member enamel-$\delta^{13}C$ values for pure C_3 and C_4 diet are −8‰ and +2‰, respectively).

The serial enamel isotope data from 4.2-Ma horses and rhinos reveal little or no intra-tooth $\delta^{13}C$ variations in individual teeth (Fig. 4). These serial enamel-$\delta^{13}C$ data indicate a diet consisting entirely of C_3 plants throughout the time interval preserved in these teeth, confirming the inference based on the bulk enamel C isotope data (Fig. 3a). In contrast, serial enamel-$\delta^{18}O$ values display significant intra-tooth variations, indicating a climate with significant seasonal variations in the $\delta^{18}O$ of local meteoric water. Carbon isotope analysis of fossil plant materials in the basin showed that C_4 grasses were present in local ecosystems in the latest Miocene and Pliocene (Saylor et al., 2009). Our enamel-$\delta^{13}C$ data, however, suggest that C_4 grasses must have been a minor component of local ecosystems at 4.2–3.1 Ma in the mid-Pliocene because they were insignificant in the herbivores' diets (Figs. 3a and 4).

The average modern-equivalent diet-$\delta^{13}C$ value of -25.3 ± 0.8‰ for the mid-Pliocene herbivores reconstructed from the enamel-$\delta^{13}C$ values is ~2‰ lower than that of modern herbivores (-23.4 ± 1.8‰) in the area (t-test, $t = 6.32$, $d.f. = 86$, M.D. = 1.9, $p < 0.0001$). However, as discussed above, three domesticated animals and a fossil bovid may have ingested a small amount of C_4 plants. Excluding data from these individuals that are suspected to have consumed some C_4 plants, the difference in $\delta^{13}C$ values between modern C_3 diets (-24.0 ± 1.6‰, $n = 11$) and modern-equivalent mid-Pliocene C_3 diets (-25.4 ± 0.7‰, $n = 73$) would decrease slightly to 1.3‰ (t-test, $t = 4.76$, $d.f. = 82$, M.D. = 1.3, $p < 0.0001$). These analyses reveal a small but significant shift to higher $\delta^{13}C$ values after the mid-Pliocene, mostly likely reflecting a change in the $\delta^{13}C$ composition of local biomass. The latter calculation above provides a conservative estimate of the magnitude of this C isotopic shift in C_3 diets in the basin. The observed increase of ~1–2‰ in the $\delta^{13}C$ of C_3 diets could be due to increased aridity and/or a change in species composition in local ecosystems caused by changes in environmental conditions.

It is well documented that C_3 plants become less depleted in the heavy C isotope ^{13}C relative to contemporary atmospheric CO_2 under water-stressed conditions (e.g., Farquhar et al., 1989; Kohn, 2010; Wang et al., 2008a). A recent analysis of a global C_3 $\delta^{13}C$ dataset demonstrates that $\delta^{13}C$ values of C_3 plants in the modern world are strongly and negatively correlated with mean annual precipitation (MAP) as defined by the following regression equation (Kohn, 2010):

$$\delta^{13}C = -10.29 + 1.90 \times 10^{-4}\,\mathrm{Altitude(m)} - 5.61\log_{10}(\mathrm{MAP} + 300,\ \mathrm{mm/yr}) - 0.0124\,\mathrm{Abs(latitude)},\quad R^2 = 0.59$$

If we assume that the above equation applied to the past and there was no significant changes in altitude and latitude of the Zanda Basin since the mid-Pliocene, the observed increase of ~1–2‰ in the $\delta^{13}C$ values of C_3 diets/biomass in the Zanda Basin would suggest a decrease in MAP in the area by ~200–400 mm since 4–3 Ma. An increased aridity in the Zanda Basin after the mid-Pliocene is also supported by the $\delta^{18}O$ data as discussed below and the fauna evidence (i.e., a rich and diverse Pliocene fauna vs. the rare and low diversity modern fauna) (Wang et al., 2013).

4.2. $\delta^{18}O$ of water and environment of mid-Pliocene fauna

The $\delta^{18}O$ values of bulk enamel structural carbonate ($\delta^{18}O_c$) from modern herbivores in the Zanda Basin are -8.7 ± 1.7‰ ($n = 14$), ranging from −7.3‰ to −12.8‰ (Fig. 3b), whereas enamel samples from the mid-Pliocene herbivores yielded a mean $\delta^{18}O_c$ value of -13.8 ± 2.9‰ ($n = 74$, with a range of −6.3‰ to −18.8‰), which is significantly lower than that of modern teeth (t-test, $t = 6.5987$, $d.f. = 86$, M.D. = 5.2, $p < 0.0001$).

Studies have shown that the $\delta^{18}O$ values of bioapatite (i.e., enamel and bone) from large mammals (>1 kg) are strongly correlated with the $\delta^{18}O$ of local meteoric water (which provides drinking water for the animals and water for plants consumed by animals), with correlation coefficient (R^2) ranging from 0.77 to 0.99 for different animals (e.g., Longinelli, 1984; Hoppe, 2006). Although the relationship may vary significantly among taxa due to differences in physiology and diet/drinking behavior of different animals, regression analyses of a global data set reveal that obligate drinkers (i.e., strongly water-dependent mammals) show a strong positive correlation between $\delta^{18}O$ of enamel/bone phosphate ($\delta^{18}O_p$) and local water ($\delta^{18}O_w$) as defined by the following equation: $\delta^{18}O_p(\mathrm{VSMOW}) = 0.96\delta^{18}O_w(\mathrm{VSMOW}) + 23$ (Kohn and Cerling, 2002). This equation can be converted to the following relationship between the $\delta^{18}O$ of structural carbonate in bioapatite ($\delta^{18}O_c$) and local water ($\delta^{18}O_w$) using the relationship between $\delta^{18}O_p$ and $\delta^{18}O_c$ for modern mammals (Iacumin et al., 1996) and the relationship between the VSMOW and VPDB reference scales (Friedman and O'Neil, 1977):

$$\delta^{18}O_w(\mathrm{VSMOW}) = \left[\delta^{18}O_c(\mathrm{VPDB}) - 1.244\right]/0.891$$

In the Himalayan–Tibetan Plateau, Wang et al. (2008b) show that the enamel-$\delta^{18}O$ values of horses and yaks are strongly correlated with the $\delta^{18}O$ of local water ($R^2 = 0.7$), displaying a regression relationship very similar to the above equation derived from a global data set by Kohn and Cerling (2002) for obligate drinkers. Using the above equation, we estimated the $\delta^{18}O$ values of modern and paleo-water from the $\delta^{18}O_c$ values of enamel from large mammals except cervid (deer) which are known to be drought-tolerant (i.e., less water-dependent) (Kohn and Cerling, 2002) (Fig. 3c).

Rain samples from the basin have $\delta^{18}O$ values ranging from −8.8‰ to −26.1‰ (Fig. 5a), with a mean of -19.8 ± 5.1‰ ($n = 14$). The rain samples collected in the summer of 2010, which was unusually wet and had more frequent and larger storms than the summer of 2007, have an average $\delta^{18}O$ value of -21.2 ± 3.8‰ ($n = 10$), which is lower than that of rain samples collected in 2007 (Supplementary Table 1). A rain sample collected in Saga (N29°19′47.1″, E85°13′49.6″, 4495 m) in August of 2010 has $\delta^{18}O$ and δD of −35.7‰ and −265.5‰, respectively, which are the lowest among all rain samples analyzed from southwest Tibet (Fig. 5a). Ponds and lakes in the Tibetan region are significantly enriched in ^{18}O relative to local meteoric water due to high evaporation which preferentially removes light isotope ^{16}O from water (Gonfiantini, 1986; Wang et al., 2008a). Modern stream waters in the Zanda Basin have $\delta^{18}O$ values, with one exception, that all fall within the isotopic range of modern precipitation in the basin and plot directly on the Global Meteoric Water Line (GMWL) as shown in Fig. 5a. This indicates that these stream waters were derived from local precipitation and had experienced little evaporation. The one exception is a stream water sample (JQ-81) from Saylor et al. (2009); it had higher $\delta^{18}O$ and δD values and plotted below the GMWL in Fig. 5a, indicating that it was significantly affected by evaporation (Gonfiantini, 1986; Wang et al., 2008a). The mean $\delta^{18}O$ value of modern streams (-14.6 ± 2.1‰) is higher than the mean $\delta^{18}O$ value of summer rains (-19.8 ± 5.1‰) (t-test, $t = 5.019$, $d.f. = 45$, M.D. = 5.2, $p < 0.0001$), reflecting mixing of melt-water from winter snows (with higher $\delta^{18}O$ values) in the streams. There is no clear elevation effect in the isotopic compositions of rain and stream waters in southwest Tibet (Fig. 5b). Our precipitation isotope data from the Zanda Basin display a large range of $\delta^{18}O$ and δD variations that appear to be controlled by the precipitation amount – the "amount effect" (Dansgaard, 1964; Johnson and Ingram, 2004;

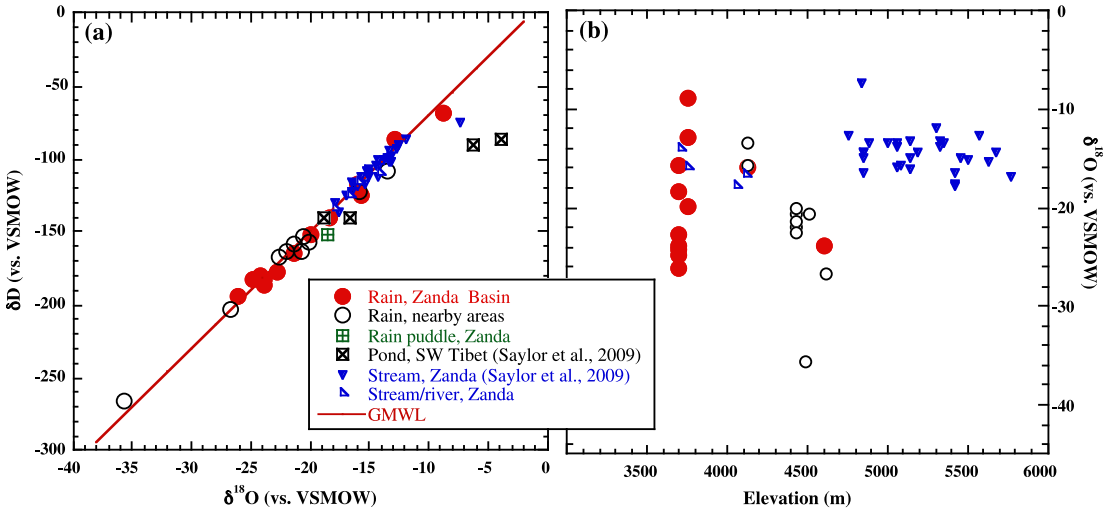

Fig. 5. Variations of $\delta^{18}O$ with δD values (a) and with elevation (b) of rains, puddle and stream waters collected in Zanda and nearby areas in the summers of 2007 and 2010. Also plotted are the water isotope data and catchment-corrected elevations from Saylor et al. (2009) for comparison. It shows that there is no clear elevation effect in the isotopic compositions of rain and stream waters in southwest Tibet.

Wang et al., 2008a), which is consistent with observations at the IAEA-GNIP (International Atomic Energy Agency Global Network for Isotopes in Precipitation) stations in China (Johnson and Ingram, 2004; Wang et al., 2008a). Although we did not measure the amount of precipitation during rain storms in the Zanda area, data from Lhasa (29.42°N, 91.08°E, 3649 m a.s.l.), which is the only IAEA-GNIP station in Tibet, show that weighted mean monthly average precipitation $\delta^{18}O$ values (for the period of 1986–1992) varied from −6.2 to −22.06‰ and are strongly negatively correlated with the precipitation amounts with an "amount effect" of 9.54‰/100 mm ($r = -0.84951$).

The estimated modern water-$\delta^{18}O$ values (based on enamel-$\delta^{18}O_c$ values of *Equus*, cow and goat) are -10.9 ± 1.9‰, ranging from −15.5 to −9.4‰ (Fig. 3c), which are within the measured $\delta^{18}O$ range of rain (and stream) waters in the Zanda Basin (Fig. 5). However, the estimated average $\delta^{18}O$ value of local water (-10.9 ± 1.9‰) is higher than the mean $\delta^{18}O$ value of modern streams (-14.6 ± 2.1‰) (*t*-test, $t = 5.828$, $d.f. = 45$, M.D. = 3.7, $p < 0.0001$). This suggests that in the present-day arid environment of the Zanda Basin herbivores rely on all available water sources (i.e., streams, rain puddles and ponds) for drinking water. Intake of water from evaporated water sources such as ponds would result in higher enamel-$\delta^{18}O$ values compared to those of precipitation. The estimated $\delta^{18}O$ values of paleo-water in the mid-Pliocene range from -13.9 ± 2.3‰ at 4.2 Ma to -19.4 ± 1.0 at ~3.8 Ma, which are significantly lower than modern water $\delta^{18}O$ values estimated from the enamel-$\delta^{18}O$ values of modern obligate drinkers (*t*-test, $t = 5.467$, $d.f. = 247$, M.D. = 4.1, $p < 0.0001$) (Fig. 3c). Based on the most negative $\delta^{18}O$ value of fossil gastropods, Saylor et al. (2009) also inferred that paleo-meteoric water in the Mio-Pliocene Zanda Basin had more negative $\delta^{18}O$ values than the present-day precipitation in the basin.

The $\delta^{18}O$ value of local water is influenced by a complex array of factors such as changes in temperature, monsoon intensity, aridity, elevation, and history and source of moisture. There is a strong positive correlation between precipitation $\delta^{18}O$ and air temperature at mid to high latitudes (Dansgaard, 1964; Rozanski et al., 1993), but this correlation is non-existent in the Asian monsoon region (Johnson and Ingram, 2004; Vuille et al., 2005). The present-day Zanda Basin is within the Indian Monsoon regime where the southwest Asian monsoon (i.e., the Indian Monsoon) provides summer precipitation in June to August. In the Asian summer monsoon region, summer precipitation has lower $\delta^{18}O$ values than winter precipitation, primarily due to the "amount effect" (Dansgaard, 1964; Johnson and Ingram, 2004; Wang et al., 2008a). The precipitation amount in the summer monsoon region is mainly controlled by the monsoon intensity (Johnson and Ingram, 2004; Vuille et al., 2005). If similar effects controlled the isotopic composition of precipitation in the Pliocene, the lower paleo-water $\delta^{18}O$ values in the mid-Pliocene would indicate a wetter climate or stronger summer monsoon 4.2–3.1 Ma than today, which is consistent with the inference from the $\delta^{13}C$ data (see previous section) and also the pollen and invertebrate fossil evidence (Bradley et al., 2006; Li and Zhou, 2001; Zhu et al., 2007).

4.3. Temperature reconstruction of mid-Pliocene Zanda Basin

We use two different approaches to provide independent estimates of paleo-temperatures in the mid-Pliocene in the Zanda Basin.

First, we used a fossil-based O isotope temperature proxy (Kohn and Law, 2006; Zanazzi et al., 2007). The premise of this approach is that the $\delta^{18}O$ of fossil bone carbonate is reset completely on time scales of tens of thousands of years during early diagenesis in soil, comparable to paleosol carbonate (Kohn and Law, 2006), whereas the $\delta^{18}O$ of enamel records the $\delta^{18}O$ of local water which is assumed to be the same as that of soil water (Kohn and Cerling, 2002; Kohn and Law, 2006; Levin et al., 2006; Wang et al., 2008a). Thus, if the $\delta^{18}O$ of local water can be estimated from the $\delta^{18}O$ of enamel, local mean annual air temperature may be estimated from the $\delta^{18}O$ of fossil bone carbonate and the $\delta^{18}O$ of local water (Kohn and Law, 2006; Zanazzi et al., 2007). Using this method, we calculated the paleo-temperatures for the mid-Pliocene Zanda Basin (Table 1) from the estimated local water $\delta^{18}O$ values (Fig. 3c), the apparent enrichment factor (~2.2‰) between bone carbonate (i.e., francolite) and soil carbonate (calcite) (Kohn and Law, 2006), and the $\delta^{18}O$ values of fossil bone carbonates (from the same time intervals) using the general oxygen isotope fractionation factor and temperature equation (Kim and O'Neil, 1997). The calculated paleo-temperatures at ~4.2–3.4 Ma in the Zanda Basin are 15 ± 7 °C, which is about 12–15 °C higher than the present-day MAT but similar to the present-day summer temperatures in the basin (Li, 2006). The uncertainty in the paleo-temperature estimate accounts for the uncertainty in the $\delta^{18}O$ variability of fossil bone carbonates. Recent studies suggest that soil/paleosol carbonates do not record the MAT but the warm

Table 1
Temperatures estimated using fossil-based oxygen isotope proxy (Kohn and Law, 2006; Zanazzi et al., 2007).

Estimated age (Ma)	Bone-δ^{18}O (VPDB)	Standard deviation	Number of bone samples	Bone-δ^{18}O (VSMOW)	Water-δ^{18}O[a] (VSMOW)	Calculated T[b] (°C)
3.4	−14.4	0.9	5	16.0	−16.1	16.5
3.5	−15.7	0.9	24	14.7	−18.4	11.9
3.6	−11.9	0.8	5	18.6	−14.9	10.1
3.8–3.9	−15.7	1.0	3	14.6	−19.4	7.6
4	−15.4	0.7	3	15.0	−15.6	23.7
4.2	−13.6	1.4	24	16.9	−13.9	22.5
					Average T:	15±7

[a] Water-δ^{18}O values were calculated from enamel-δ^{18}O values using the enamel–water δ^{18}O relationship for obligate drinkers give in Kohn and Cerling (2002) (Fig. 3c).
[b] Temperatures were calculated using the oxygen isotope fractionation factor and temperature equation of Kim and O'Neil (1997).

season temperatures (Breecker et al., 2009; Passey et al., 2010; Quade et al., 2011, 2013). Thus, the temperatures estimated from the fossil bone carbonates may be biased toward the warm season. Alternatively, if the isotopic compositions of the bones are not completely reset during early diagenesis, the bone-based paleotemperature estimates would give artificially high values, in the direction of mammalian body temperature of ~37 °C.

Second, we determined carbonate clumped isotope paleotemperatures from Pliocene fossil shells. Carbonate clumped isotope thermometry is based on the thermodynamic preference of rare isotopes of carbon (^{13}C) and oxygen (^{18}O) to bond or "clump" with each other (^{13}C–^{18}O) in carbonate-containing minerals (Ghosh et al., 2006). Unlike the conventional O isotope thermometer, clumped isotope (Δ_{47}) thermometry does not require knowledge or assumptions about the O isotope composition of the water from which a mineral was formed (Ghosh et al., 2006). The dependence of carbonate Δ_{47} value on formation temperature allows reconstruction of formation temperatures of carbonate minerals and the δ^{18}O value of water in which the shells grew (Eiler, 2007; Ghosh et al., 2006; Passey et al., 2010).

The lacustrine strata in the Zanda Basin contain abundant fossil shells of several extinct freshwater snails (Han et al., 2012). We determined clumped isotope compositions (Δ_{47}) of four mid-Pliocene fossil shells (Table 2). The shells analyzed represent two extinct species: *Veletinopsis spiralis* Yu (belonging to the Lymnaeidae family) and *Radix zandaensis* sp. nov. (in the Physidae family) (Supplementary Fig. 1). Both species are thought to have lived in a shallow littoral lake environment in a warm and wet climate (Han et al., 2012). There are significant discrepancies between existing calibration equations used to derive temperatures from measured Δ_{47} values, which leads to discrepancies in the calculated paleotemperatures and paleo-water δ^{18}O values. For example, the Δ_{47} value of the 4-Ma sample TB07s-6a (0.700‰) results in a temperature of 13.6°C and a water-δ^{18}O value of −4.7‰ using the inorganic carbonate calibration (Ghosh et al., 2006), a temperature of 11.3 °C and a water-δ^{18}O value of −5.3‰ using an otolith + marine shell calibration (Came et al., 2007; Ghosh et al., 2006), and a temperature of 0.0 °C and a water-δ^{18}O value of −7.8‰ using a new marine shell calibration (Henkes et al., 2013) (Table 2). Although the fossil snails analyzed are all extinct, their modern relatives are widespread in south China (Han et al., 2012), and *Radix* sp. are also found in freshwater and oligohaline to mesohaline lakes on the present-day Himalayan–Tibetan Plateau (Taft et al., 2012). The life span of modern *Radix* snails in Tibet is approximately one year; they either remain active under ice cover or move from the shallow littoral area to deeper water during winter months (Taft et al., 2013). Their shells continue to grow but at much slower rates in the winter, recording sub-seasonal variations in their environmental conditions (Taft et al., 2012, 2013). If the extinct snails had a similar life cycle as their modern relatives, temperatures derived from their shells would be biased towards the warmer seasons when water temperatures are above 0 °C. Seasonal bias is also seen in terrestrial gastropods and marine bivalves from temperate settings (Henkes et al., 2013; Zaarur et al., 2011). In this context, the essentially freezing mean temperature given by the Henkes et al. (2013) calibration (−0.7 ± 4.2 °C) seems unreasonable. The temperatures derived from the inorganic calibration (Ghosh et al., 2006) are very similar to the present-day summer temperatures in the area and also close to the temperature estimates based on the O isotopic compositions of fossil bones and enamel as discussed above. The temperatures calculated using the otolith and marine shell calibration (Came et al., 2007; Ghosh et al., 2006) are ~2 °C lower than those derived from the inorganic calibration and fall in between the present MAT (0–3 °C) and summer temperature (~13–14 °C). The inconsistencies among the Δ_{47}-based temperatures (and water-δ^{18}O values) derived from different calibrations are being further investigated, and may relate to analytical differences, or real differences in 'vital' effects. We note that there are no existing calibrations for freshwater mollusks similar to those studied here, and in further discussion we consider only the temperatures calculated using calibrations from the Ghosh et al. (2006) and Came et al. (2007) data, which yielded an average temperature of 12 ± 3 °C for the mid-Pliocene Zanda Basin.

The water-δ^{18}O values calculated from the temperatures derived from inorganic calibration (Ghosh et al., 2006) and the otolith and marine shell calibration (Came et al., 2007; Ghosh et al., 2006) are −4.4 ± 0.4‰ and −4.9 ± 0.4‰, respectively (Table 2). These calculated water-δ^{18}O values are significantly higher than the average water-δ^{18}O value derived from enamel-δ^{18}O values, which is expected for evaporated lake water as evaporation preferentially removes isotopically lighter water molecules leaving remaining water enriched in ^{18}O relative to meteoric water (e.g., Gonfiantini, 1986; Wang et al., 2008b). Although there are no lakes in the Zanda Basin today for direct comparison, the estimated paleo-lake water δ^{18}O values are comparable to those of freshwater (or low salinity) lakes in the region (Supplementary Table 1).

4.4. Paleo-elevation implications

Previous studies on the fossil floral and faunal assemblages found in the Zanda Formation suggest warmer and more humid climates and by inference lower elevation environments in the Pliocene Zanda Basin than today (Han et al., 2012; Li and Zhou, 2001, 2002; Zhu et al., 2007; 2004), although long-distance transport of pollen may bias pollen assemblages toward compositions in surrounding regions (Song et al., 2010). More recent studies (Murphy et al., 2009; Saylor et al., 2009), based on the δ^{18}O values of fossil shells, suggest that the Zanda Basin stood as high as, and possibly up to 1.5 km higher than today, and that the environment in the basin has been as arid as today since at least 9 Ma, which is in stark contrast to the inference from the fossil evidence (Li and Zhou, 2001, 2002; Zhu et al., 2007, 2004). Using the present-day atmospheric lapse rate of −6.5 °C/km, an

Table 2
Temperatures and water-$\delta^{18}O$ values calculated using carbonate clumped isotope thermometry on fossil shells.

Sample ID	Locality	Estimated age (Ma)	$\delta^{13}C$ (vs. VPDB)	$\delta^{18}O$ (vs. VPDB)	Δ_{47} (‰)	T (°C)[a] (inorganic calibration)	Calculated $\delta^{18}O$ of water (‰ vs. VSMOW)	T (°C)[b] (shells + otolith calibration)	Calculated $\delta^{18}O$ of water (‰ vs. VSMOW)	T (°C)[c] (new JHU mollusk-specific calibration)	Calculated $\delta^{18}O$ of water (‰ vs. VSMOW)	Elevation (m)	Present-day[d] MAT (°C)
ZD0710	Zanda	3.7	−0.13	−2.85	0.708	12.1	−4.0	9.6	−4.5	−2.6	−7.4	4212	0–1
TB07S-6	Zanda	4	−0.65	−3.25	0.716	10.6	−4.7	7.9	−5.3	−5.0	−8.4	4190	0–1
TB07S-6a	Zanda	4	−2.36	−3.93	0.700	13.6	−4.7	11.3	−5.3	0.0	−7.8	4190	0–1
TB07S-19a	Zanda	4.4	−0.46	−4.03	0.685	16.6	−4.2	14.4	−4.7	4.9	−6.8	4123	0–1
					Average ±1 sigma	13.2 (°C) ±2.6	−4.4 (‰) ±0.4	10.8 (°C) ±2.8	−4.9 (‰) ±0.4	−0.7 (°C) ±4.2	−7.6 (‰) ±0.7		

Values are reported relative to the 'heated gas' scale (Ghosh et al., 2006; Huntington et al., 2009). Uncertainty is ±0.025‰ (95% confidence interval), which is the long-term 95% confidence interval for repeated analyses of homogeneous in-house carbonate standards at Johns Hopkins University.

[a] Temperatures calculated from Δ_{47} data using inorganic carbonate calibration (Ghosh et al., 2006): $\Delta_{47} = 59200/T^2 - 0.02$. Uncertainty in reported temperatures is ±5.0 °C (95% confidence interval).

[b] Temperatures calculated from Δ_{47} data using a 'shell/otolith' calibration based on the combined datasets of Ghosh et al. (2006) and Came et al. (2007): $\Delta_{47} = 53\,363/T^2 + 0.04$. Uncertainty in reported temperatures is ±5.4 °C (95% confidence interval).

[c] Temperatures calculated from Δ_{47} data using a new mollusk-specific calibration (Henkes et al., 2013): $\Delta_{47} = 31\,800/T^2 + 0.2737$. Uncertainty in reported temperatures for individual shells is ±8.4 °C (95% confidence interval).

[d] Mean annual temperatures were calculated using the temperature–elevation equation (i.e., T (°C) = −0.0081 × Elev + 35.326) for the region (Quade et al., 2011).

elevation change of 1.5 km would be equivalent to a temperature change of ∼10 °C. That is, if the Zanda Basin was indeed 1.5 km higher in the Mio-Pliocene than today (Murphy et al., 2009; Saylor et al., 2009), its MAT in the Mio-Pliocene would be about −10 °C (i.e., ∼10 °C lower than today) assuming no significant change in global temperature since the Mio-Pliocene. Such low MAT seems unlikely given the abundance and diversity of fossil mammals, fish and shells found in the late Miocene–Pliocene strata and the existence of warm climate C_4 grasses in the basin as revealed by C isotope analysis of fossil plant material (Saylor et al., 2010b, 2009). Furthermore, an increase of 1.5 km would elevate much of the paleo-Zanda Basin above 5500 m a.s.l., an elevation at which few modern vegetation can survive (Schaller, 1998).

Our enamel C isotope data show that C_4 grasses were not a significant component of herbivores' diets and local ecosystems in the mid-Pliocene Zanda Basin and that the biomass in the area has been dominated by C_3 vegetation since ∼4.2 Ma. In the modern ecosystems, C_4 grasses are mostly confined to low altitudes: < 2500 m in mid latitudes and < 3000 m in the tropics (Boutton et al., 1980; Edwards et al., 2010; Hofstra et al., 1972; Li et al., 2009; Tieszen et al., 1979). Although C_4 grasses have been found in the warmest months in southern Tibet, they account for negligible amounts of the biomass (Li et al., 2009; Lu et al., 2004; Wang et al., 2008a). The lack of significant C_4 biomass in the Zanda Basin at 4.2–3.1 Ma suggests that the elevation of the basin was at least higher than 2500 m a.s.l. in the mid-Pliocene.

We estimated the paleo-temperatures for mid-Pliocene Zanda Basin using two independent methods (see previous section). The paleo-temperature estimates derived from the fossil-based O isotope temperature proxy are 15 ± 7 °C, whereas the paleo-temperatures determined from the "clumped" isotope (Δ_{47}) analysis are 12 ± 3 °C. These temperatures are significantly higher than the present-day MAT of ∼0–3 °C in the area. Marine paleo-temperature records suggest that the ocean temperatures in the Pliocene warm period (5–3 Ma) were about 2–3 °C higher than today (Lear et al., 2000; Ravelo et al., 2004). Temperature change at high elevations is likely larger than at sea level (Bradley et al., 2006). If we assume that late Cenozoic global cooling has resulted in a temperature drop of 5 °C (about twice that at sea level) in the Zanda Basin since ∼4–3 Ma and the temperatures derived from "clumped" isotope (Δ_{47}) analyses of shells most closely approximate the MAT, the estimated local temperature change (6 ± 3 °C) in the basin would suggest an elevation change of 923 ± 462 m since the mid-Pliocene using the present-day atmospheric temperature lapse rate of −6.5 °C/km. In other words, the paleo-elevation of the Zanda Basin at 4–3 Ma was ∼3277 ± 462 m a.s.l. close to its present-day elevation (∼4200 m a.s.l.). However, in the case that shell growth was biased towards the warm seasons (when water temperatures are above 0 °C) as discussed in the previous section, the actual difference in MAT between now and the mid-Pliocene would be smaller than computed above, and hence the elevation difference would also be smaller. Similarly, if we assume that the paleo-temperatures derived from the fossil-based O isotope proxy approximate the MAT and the local temperature change due to global cooling was 5 °C, the estimated temperature change (∼9 °C) would correspond to an elevation change of 1385 ± 1077 m, implying that the paleo-elevation of the mid-Pliocene Zanda Basin was 2815 ± 1077 m. However, as discussed in the previous section, the temperatures derived from the fossil-based O isotope proxy are likely biased toward the warm season temperatures. Assuming warm season air temperatures were about 6 °C higher than the MAT as suggested by the long-term modern climate records in Lhasa, the estimated change of local MAT would be ∼4 °C since the mid-Pliocene after accounting for local temperature change due to global cooling, which is equivalent to an elevation change of 615 ± 1077 m and

implies a paleo-elevation of $\sim 3585 \pm 1077$ m a.s.l. for the mid-Pliocene Zanda Basin, slightly lower than the present-day elevation of the basin. Despite large uncertainties, elevation estimates derived from two different temperature proxies all suggest that the paleo-elevation of the Zanda Basin in the mid-Pliocene was similar to its present-day elevation, which is consistent with the C isotope data and also the fossil evidence (Bradley et al., 2006; Deng et al., 2012, 2011).

5. Conclusions

- The enamel-$\delta^{13}C$ data indicate that the mid-Pliocene mammalian fauna in the Zanda Basin, like modern herbivores in the area, fed primarily on C_3 vegetation and lived in an environment dominated by C_3 plants. The lack of significant C_4 plants in the basin suggests that the elevation of the area in the mid-Pliocene was higher than 2.5 km.
- The estimated $\delta^{18}O$ values of paleo-water in the mid-Pliocene Zanda Basin were lower than those of modern surface waters in the basin, most likely indicating a shift in climate to much drier conditions after $\sim$4–3 Ma.
- The enamel-$\delta^{13}C$ values also reveal that the average modern-equivalent $\delta^{13}C$ value (i.e., corrected for the change in the $\delta^{13}C$ of atmospheric CO_2) of C_3 biomass at 4.2–3.1 Ma is about 1–2‰ lower than that of modern C_3 vegetation in the basin, implying that the annual precipitation in the mid-Pliocene was likely $\sim$200–400 mm higher than today, consistent with a wetter climate as inferred from the enamel-$\delta^{18}O$ data.
- Paleo-temperatures estimated using two different methods suggest that the Zanda Basin had a warmer climate and was at a similar or slightly lower elevation at 4.2–3.1 Ma than today, consistent with the inference from the $\delta^{13}C$ data.

Acknowledgements

This study was supported by grants from the U.S. National Science Foundation (EAR0444073 and EAR0958602 to Y.W., EAR-0446699 and EAR0958704 to X.W.), Chinese Academy of Sciences (XDB03020104) and National Natural Science Foundation of China (40730210, 40702004). Isotope analyses of teeth and water were performed at the Florida State University Stable Isotope Laboratory supported by grants from the U.S. National Science Foundation (EAR0517806). "Clumped isotope" measurements were performed in Dr. John Eiler's Lab at California Institute of Technology. Dr. Passey's post-doc work in Dr. Eiler's lab was supported by the Dreyfus Foundation. We thank two anonymous reviewers for helpful suggestions and comments.

Appendix A. Supplementary material

Supplementary material related to this article can be found online at http://dx.doi.org/10.1016/j.epsl.2013.06.014.

References

An, Z., Kutzbach, J.E., Prell, W.L., Porter, S.C., 2001. Evolution of Asian monsoons and phased uplift of the Himalayan Tibetan plateau since Late Miocene times. Nature 411, 62–66.

Boutton, T.W., Harrison, A.T., Smith, B.N., 1980. Distribution of biomass of species differing in photosynthetic pathway along an altitudinal transect in southeastern Wyoming grassland. Oecologia 45, 287–298.

Bradley, R.S., Vuille, M., Diaz, H.F., Vergara, W., 2006. Threats to water supplies in the tropical Andes. Science 312, 1755–1756.

Breecker, D.O., Sharp, Z.D., McFadden, L.D., 2009. Seasonal bias in the formation and stable isotopic composition of pedogenic carbonate in modem soils from central New Mexico, USA. Geol. Soc. Am. Bull. 121, 630–640.

Came, R.E., Eiler, J.M., Veizer, J., Azmy, K., Brand, U., Weidman, C.R., 2007. Coupling of surface temperatures and atmospheric CO_2 concentrations during the Palaeozoic era. Nature 449, 193–198.

Cerling, T.E., Harris, J., MacFadden, B., Leakey, M., Quade, J., Eisenmann, V., Ehleringer, J., 1997. Global vegetation change through the Miocene/Pliocene boundary. Nature 389, 153–158.

Cuntz, M., 2011. Carbon cycle: A dent in carbon's gold standard. Nature 477, 547–548.

Currie, B.S., Rowley, D.B., Tabor, N.J., 2005. Middle Miocene paleoaltimetry of southern Tibet: Implications for the role of mantle thickening and delamination in the Himalayan orogen. Geology 33, 181–184.

Cyr, A.J., Currie, B.S., Rowley, D.B., 2005. Geochemical evaluation of Fenghuoshan Group lacustrine carbonates, North–Central Tibet: Implications for the paleoaltimetry of the Eocene Tibetan Plateau. J. Geol. 113, 517–533.

Dansgaard, W., 1964. Stable isotopes in precipitation. Tellus 16, 436–468.

DeCelles, P.G., Quade, J., Kapp, P., Fan, M.J., Dettman, D.L., Ding, L., 2007. High and dry in central Tibet during the Late Oligocene. Earth Planet. Sci. Lett. 253, 389–401.

Deng, T., Wang, X.M., Fortelius, M., Li, Q., Wang, Y., Tseng, Z.J.J., Takeuchi, G.T., Saylor, J.E., Saila, L.K., Xie, G.P., 2011. Out of Tibet: Pliocene woolly rhino suggests high-plateau origin of ice age megaherbivores. Science 333, 1285–1288.

Deng, T., Li, Q., Tseng, Z., Takeuchi, G., Wang, Y., Xie, G., Wang, S., Hou, S., Wang, X., 2012. Locomotive implication of a Pliocene three-toed horse skeleton from Tibet and its paleo-altimetry significance. Proc. Natl. Acad. Sci. 109, 7374–7378.

Dennis, K.J., Affek, H.P., Passey, B.H., Schrag, D.P., Eiler, J.M., 2011. Defining an absolute reference frame for 'clumped' isotope studies of CO2. Geochim. Cosmochim. Acta 75, 7117–7131.

Dupont-Nivet, G., Krijgsman, W., Langereis, C.G., Abels, H.A., Dai, S., Fang, X.M., 2007. Tibetan plateau aridification linked to global cooling at the Eocene–Oligocene transition. Nature 445, 635–638.

Dupont-Nivet, G., Hoorn, C., Konert, M., 2008. Tibetan uplift prior to the Eocene–Oligocene climate transition: Evidence from pollen analysis of the Xining Basin. Geology 36, 987–990.

Edwards, E.J., Osborne, C.P., Stromberg, C.A.E., Smith, S.A., Bond, W.J., Christin, P.A., Cousins, A.B., Duvall, M.R., Fox, D.L., Freckleton, R.P., Ghannoum, O., Hartwell, J., Huang, Y.S., Janis, C.M., Keeley, J.E., Kellogg, E.A., Knapp, A.K., Leakey, A.D.B., Nelson, D.M., Saarela, J.M., Sage, R.F., Sala, O.E., Salamin, N., Still, C.J., Tipple, B., Consortium, C.G., 2010. The origins of C(4) grasslands: Integrating evolutionary and ecosystem science. Science 328, 587–591.

Eiler, J.M., 2007. "Clumped-isotope" geochemistry – The study of naturally-occurring, multiply-substituted isotopologues. Earth Planet. Sci. Lett. 262, 309–327.

Farquhar, G.D., Ehleringer, J.R., Hubick, K.T., 1989. Carbon isotope discrimination and photosynthesis. Ann. Rev. Plant Physiol. Plant Mol. Biol. 40, 503–537.

Friedman, I., O'Neil, J.R., 1977. Compilation of stable isotope fractionation factors of geochemical interest. In: Fleischer, M. (Ed.), Data of Geochemistry. 6th edition. U.S. Geological Survey, Reston (12 pp. and 49 figures).

Garzione, C.N., Dettman, D.L., Quade, J., DeCelles, P.G., Butler, R.F., 2000. High times on the Tibetan Plateau: Paleoelevation of the Thakkhola graben, Nepal. Geology 28, 339–342.

Ghosh, P., Adkins, J., Affek, H., Balta, B., Guo, W.F., Schauble, E.A., Schrag, D., Eller, J.M., 2006. (13)C–(18)O bonds in carbonate minerals: A new kind of paleothermometer. Geochim. Cosmochim. Acta 70, 1439–1456.

Gonfiantini, R., 1986. Environmental isotopes in lake studies. In: Handbook of Environmental Isotope Geochemistry: The Terrestrial Environment. Elsevier, Amsterdam, The Netherlands, pp. 113–168.

Graham, S.A., Chamberlain, C.P., Yue, Y.J., Ritts, B.D., Hanson, A.D., Horton, T.W., Waldbauer, J.R., Poage, M.A., Feng, X., 2005. Stable isotope records of Cenozoic climate and topography, Tibetan plateau and Tarim basin. Am. J. Sci. 305, 101–118.

Han, J., Xu, J., He, C., Meng, Q., Zhu, D., Meng, X., Shao, Z., Yang, C., 2012. The assemblage of gastropod fossils in Zanda Basin of Tibet and its biostratigraphy. Acta Geosci. Sin. 33, 153–166.

Harrison, T.M., Copeland, P., Kidd, W.S.F., Yin, A., 1992. Raising Tibet. Science 255, 1663–1670.

Henkes, G.A., Passey, B.H., Wanamaker, A.D., Grossman, E.L., Ambrose, W.G., Carroll, M.L., 2013. Carbonate clumped isotope compositions of modern marine mollusk and brachiopod shells. Geochim. Cosmochim. Acta 106, 307–325.

Hofstra, J., Aksornkoae, S., Atmowidjojo, S., Banaag, J., Santosa, R., Sastrohoetomo, A., Thu, L., 1972. A study on the occurrence of plants with a low CO2 compensation point in different habitats in the tropics. Ann. Bogorienses 5, 143–157.

Hoppe, K., 2006. Correlation between the oxygen isotope ratio of North American bison teeth and local waters: Implications for paleoclimatic reconstructions. Earth Planet. Sci. Lett. 244, 408–417.

Huntington, K.W., Eiler, J.M., Affek, H.P., Guo, W., Bonifacie, M., Yeung, L.Y., Thiagarajan, N., Passey, B., Tripati, A., Daeron, M., Came, R., 2009. Methods and limitations of 'clumped' CO(2) isotope (Delta(47)) analysis by gas-source isotope ratio mass spectrometry. J. Mass Spectrom. 44, 1318–1329.

Iacumin, P., Bocherens, H., Mariotti, A., Longinelli, A., 1996. Oxygen isotope analyses of co-existing carbonate and phosphate in biogenic apatite: a way to monitor diagenetic alteration of bone phosphate? Earth Planet. Sci. Lett. 142, 1–6.

Johnson, K.R., Ingram, B.L., 2004. Spatial and temporal variability in the stable isotope systematics of modern precipitation in China: Implications for paleoclimate reconstructions. Earth Planet. Sci. Lett. 220, 365–377.

Kim, S.T., O'Neil, J.R., 1997. Equilibrium and nonequilibrium oxygen isotope effects in synthetic carbonates. Geochim. Cosmochim. Acta 61, 3461–3475.
Kohn, M.J., 2010. Carbon isotope compositions of terrestrial C3 plants as indicators of (paleo)ecology and (paleo)climate. Proc. Natl. Acad. Sci. USA 107, 19691–19695.
Kohn, M.J., Cerling, T.E., 2002. Stable isotope compositions of biological apatite. In: Phosphates: Geochemical, Geobiological, and Materials Importance. In: Rev. Mineral. Geochem., vol. 48, pp. 455–488.
Kohn, M.J., Law, J.M., 2006. Stable isotope chemistry of fossil bone as a new paleoclimate indicator. Geochim. Cosmochim. Acta 70, 931–946.
Lear, C.H., Elderfield, H., Wilson, P.A., 2000. Cenozoic deep-sea temperatures and global ice volumes from Mg/Ca in benthic foraminiferal calcite. Science 287, 269–272.
Levin, N.E., Cerling, T.E., Passey, B.H., Harris, J.M., Ehleringer, J.R., 2006. A stable isotope aridity index for terrestrial environments. Proc. Natl. Acad. Sci. USA 103, 11201–11205.
Li, Y.Z., 2006. Xizang Annual. Xizang People Press.
Li, J., Zhou, Y., 2001. Pliocene palynoflora from the Zanda Basin west Xizang (Tibet), and the palaeoenvironment. Acta Micropalaeontol. Sin. 18, 89–96.
Li, J., Zhou, Y., 2002. Palaeovegetation type analysis of the late Pliocene in Zanda basin of Tibet. J. Palaeogeogr. 4, 52–58.
Li, J.Z., Wang, G.A., Liu, X.Z., Han, J.M., Liu, M., Liu, X.J., 2009. Variations in carbon isotope ratios of C(3) plants and distribution of C(4) plants along an altitudinal transect on the eastern slope of Mount Gongga. Sci. China Ser. D 52, 1714–1723.
Longinelli, A., 1984. Oxygen isotopes in mammal bone phosphate – a new tool for paleohydrological and paleoclimatological research. Geochim. Cosmochim. Acta 48, 385–390.
Lourens, L., Hilgren, F., Shackleton, N.J., Laskar, J., Wilson, J., 2004. The Neogene period. In: Gradstein, F.M., Ogg, J.G., Smith, A.G. (Eds.), A Geologic Time Scale 2004. Cambridge University Press, Cambridge, pp. 409–440.
Lu, H.Y., Wu, N.Q., Gu, Z.Y., Guo, Z.T., Wang, L., Wu, H.B., Wang, G., Zhou, L.P., Han, J.M., Liu, T.S., 2004. Distribution of carbon isotope composition of modern soils on the Qinghai–Tibetan Plateau. Biogeochemistry 70, 273–297.
Meng, X., Zhu, D., Shao, Z., Yang, C., Sun, L., Wang, J., Han, T., Du, J., Han, J., Yu, J., 2004. Discovery of rhinoceros fossils in the Pliocene in the Zanda basin, Ngari area, Tibet. Geol. Bull. China 23, 609–612.
Molnar, P., 2005. Mio-Pliocene growth of the Tibetan Plateau and evolution of East Asian climate. Palaeontol. Electron. 8 (1), 1–23.
Molnar, P., England, P., Martinod, J., 1993. Mantle dynamics, uplift of the Tibetan Plateau, and the Indian monsoon. Rev. Geophys. 31, 357–396.
Murphy, M.A., Saylor, J.E., Ding, L., 2009. Late Miocene topographic inversion in southwest Tibet based on integrated paleoelevation reconstructions and structural history. Earth Planet. Sci. Lett. 282, 1–9.
O'Leary, M.H., 1988. Carbon isotopes in photosynthesis. Bioscience 38, 328–336.
Passey, B.H., Levin, N.E., Cerling, T.E., Brown, F.H., Eiler, J.M., 2010. High-temperature environments of human evolution in East Africa based on bond ordering in paleosol carbonates. Proc. Natl. Acad. Sci. USA 107, 11245–11249.
Quade, J., Breecker, D.O., Daeron, M., Eiler, J., 2011. The paleoaltimetry of Tibet: An isotopic perspective. Am. J. Sci. 311, 77–115.
Quade, J., Eiler, J., Daeron, M., Achyuthan, H., 2013. The clumped isotope geothermometer in soil and paleosol carbonate. Geochim. Cosmochim. Acta 105, 92–107.
Ravelo, A.C., Andreasen, D.H., Lyle, M., Lyle, A.O., Wara, M.W., 2004. Regional climate shifts caused by gradual global cooling in the Pliocene epoch. Nature 429, 263–267.
Raymo, M.E., Ruddiman, W.F., 1992. Tectonic forcing of late Cenozoic climate. Nature 359, 117–122.
Rowley, D.B., Currie, B.S., 2006. Palaeo-altimetry of the late Eocene to Miocene Lunpola basin, central Tibet. Nature 439, 677–681.
Rowley, D.B., Garzione, C.N., 2007. Stable isotope-based paleoaltimetry. Annu. Rev. Earth Planet. Sci. 35, 463–508.
Rowley, D.B., Pierrehumbert, R.T., Currie, B.S., 2001. A new approach to stable isotope-based paleoaltimetry: implications for paleoaltimetry and paleohypsometry of the High Himalaya since the Late Miocene. Earth Planet. Sci. Lett. 188, 253–268.
Rozanski, K., Araguas-Araguas, L., Gonfiantini, R., 1993. Isotopic patterns in modern global precipitation. In: Swart, P., Lohmann, K., McKenzie, J., Savin, S. (Eds.), Climate Change in Continental Isotopic Records. In: American Geophysical Union Geophysical Monographs. AGU, Washington, DC, pp. 1–36.
Ruddiman, W.F., Raymo, M.E., Prell, W., Kutzbach, J.E., 1997. The uplift-climate connection: A synthesis. In: Ruddiman, W.F. (Ed.), Tectonic Uplift and Climate Change. Plenum Press, New York, pp. 471–515.
Saylor, J., Quade, J., Dettman, D., DeCelles, P., Kapp, P., Ding, L., 2009. The late Miocene through present paleoelevation history of southwestern Tibet. Am. J. Sci. 309, 1–42.
Saylor, J., DeCelles, P., Gehrels, G., Murphy, M., Zhang, R., Kapp, P.A., 2010a. Basin formation in the high Himalaya by arc-parallel extension and tectonic damming: Zhada Basin, southwestern Tibet. Tectonics 29, TC1004.
Saylor, J., DeCelles, P., Quade, J., 2010b. Climate-driven environmental change in the Zhada Basin, southwestern Tibetan Plateau. Geosphere 6, 74–92.
Schaller, G.B., 1998. Wildlife of the Tibetan Steppe. University of Chicago, Chicago.
Song, X.Y., Spicer, R.A., Yang, J.A., Yao, Y.F., Li, C.S., 2010. Pollen evidence for an Eocene to Miocene elevation of central southern Tibet predating the rise of the High Himalaya. Palaeogeogr. Palaeoclimatol. Palaeoecol. 297, 159–168.
Spicer, R.A., Harris, N.B.W., Widdowson, M., Herman, A.B., Guo, S.X., Valdes, P.J., Wolfe, J.A., Kelley, S.P., 2003. Constant elevation of southern Tibet over the past 15 million years. Nature 421, 622–624.
Sun, L.M., Yan, T.S., Tang, G.Y., Ding, X.Y., Wang, R.J., Tian, L.F., 2007. Neogene sporopollen assemblages and paleography in the Gyirong basin, Tibet. Geol. China 34, 49–54.
Taft, L., Wiechert, U., Riedel, F., Weynell, M., Zhang, H.C., 2012. Sub-seasonal oxygen and carbon isotope variations in shells of modern Radix sp (Gastropoda) from the Tibetan Plateau: potential of a new archive for palaeoclimatic studies. Quat. Sci. Rev. 34, 44–56.
Taft, L., Wiechert, U., Zhang, H., Lei, G., Mischke, S., Plessen, B., Weynell, M., Winkler, A., Riedel, F., 2013. Oxygen and carbon isotope patterns archived in shells of the aquatic gastropod Radix: Hydrologic and climatic signals across the Tibetan Plateau in sub-monthly resolution. Quat. Int. 290–291, 282–298.
Tian, L., Masson-Delmotte, V., Stievenard, M., Yao, T., Jouzel, J., 2001. Tibetan Plateau summer monsoon northward extent revealed by measurements of water stable isotopes. J. Geophys. Res., Atmos. 106, 28081–28088.
Tian, L.D., Yao, T.D., White, J.W.C., Yu, W.S., Wang, N.L., 2005. Westerly moisture transport to the middle of Himalayas revealed from the high deuterium excess. Chin. Sci. Bull. 50, 1026–1030.
Tieszen, L.L., Hein, D., Qvortrup, S.A., Troughton, J.H., Imbamba, S.K., 1979. Use of $\delta^{13}C$ values to determine vegetation selectivity in East African herbivores. Oecology 37, 351–359.
Tipple, B.J., Meyers, S.R., Pagani, M., 2010. Carbon isotope ratio of Cenozoic CO(2): A comparative evaluation of available geochemical proxies. Paleoceanography 25, PA3202, 1–11.
Vuille, M., Werner, M., Bradley, R.S., Keimig, F., 2005. Stable isotopes in precipitation in the Asian monsoon region. J. Geophys. Res., Atmos. 110.
Wang, W., 2004. Structural and sedimentary features in Zanda Basin of Tibet. Acta Sci. Natur. 40, 872–878.
Wang, Y., Deng, T., 2005. A 25 m.y. isotopic record of paleodiet and environmental change from fossil mammals and paleosols from the NE margin of the Tibetan Plateau. Earth Planet. Sci. Lett. 236, 322–338.
Wang, Y., Deng, T., Biasatti, D., 2006. Ancient diets indicate significant uplift of southern Tibet after ca. 7 Ma. Geology 34, 309–312.
Wang, Y., Kromhout, E., Zhang, C.F., Xu, Y.F., Parker, W., Deng, T., Qiu, Z.D., 2008a. Stable isotopic variations in modern herbivore tooth enamel, plants and water on the Tibetan Plateau: Implications for paleoclimate and paleoelevation reconstructions. Palaeogeogr. Palaeoclimatol. Palaeoecol. 260, 359–374.
Wang, Y., Wang, X.M., Xu, Y.F., Zhang, C.F., Li, Q., Tseng, Z.J., Takeuchi, G., Deng, T., 2008b. Stable isotopes in fossil mammals, fish and shells from Kunlun Pass Basin, Tibetan Plateau: Paleo-climatic and paleo-elevation implications. Earth Planet. Sci. Lett. 270, 73–85.
Wang, Y., Deng, T., Flynn, L., Wang, X., An, Y., Xu, Y., Parker, W., Lochner, E., Zhang, C., Biasatti, D., 2012. Late Neogene environmental changes in the central Himalaya related to tectonic uplift and orbital forcing. J. Asian Earth Sci. 44, 62–76.
Wang, X.M., Li, Q., Xie, G., Saylor, J., Tseng, Z.J., Takeuchi, G., Deng, T., Wang, Y., Hou, S., Liu, J., Zhang, C., Wang, N., Wu, F., 2013. Mio-Pleistocene Zanda Basin biostratigraphy and geochronology, pre-Ice Age fauna, and mammalian evolution in western Himalaya. Palaeogeogr. Palaeoclimatol. Palaeoecol. 374, 81–95.
Xu, R., 1981. Vegetational changes in the past and the uplift of the Qinghai–Xizang Plateau. In: Geological and Ecological Studies of Qinghai–Xizang Plateau, vol. 1. Geology, Geological History and Origin of Qinghai–Xizang Plateau. Science Press, Beijing.
Xu, Y., Zhang, K., Wang, G., Jiang, S., Chen, F., Xiang, S., Dupont-Nivet, G., Hoorn, C., 2012. Extended stratigraphy, palynology and depositional environments record the initiation of the Himalayan Gyirong Basin (Neogene China). J. Asian Earth Sci. 44, 77–93.
Zaarur, S., Olack, G., Affek, H.P., 2011. Paleo-environmental implication of clumped isotopes in land snail shells. Geochim. Cosmochim. Acta 75, 6859–6869.
Zanazzi, A., Kohn, M.J., MacFadden, B.J., Terry, D.O., 2007. Large temperature drop across the Eocene–Oligocene transition in central North America. Nature 445, 639–642.
Zhang, Q., Wang, F., Ji, H., Huang, W., 1981. Pliocene sediments of the Zanda basin: Tibet. J. Stratigraphy 5, 216–220.
Zhou, Y., Ding, L., Deng, W., Zhang, J., 2000. Tectonic cyclothems in the Zanda Basin and its significance. Scientia Geological Sinica 35, 305–315.
Zhu, D., Meng, X., Shoa, Z., Yang, C., Sun, L., Wang, J., Han, T., Han, J., Du, J., Meng, Q., 2004. Features of Pliocene-lower Pleistocene sedimentary facies and tectonic evolution in the Zanda Basin, Ngari area: Tibet. J. Geomech. 110, 245–252.
Zhu, D., Meng, X., Shoa, Z., Yang, C., Han, J., Yu, J., Meng, Q., Lu, R., 2007. Evolution of the paleovegetation, paleoenvironment and paleoclimate during Pliocene–early Pleistocene in Zhada Basin, Ali, Tibet. Acta Geol. Sin. 81, 295–306.